

# Helix-Forming Propensity of Aliphatic Urea Oligomers Incorporating Noncanonical Residue Substitution Patterns

Nagendar Pendem,<sup>†,⊥</sup> Céline Douat,<sup>†</sup> Paul Claudon,<sup>†</sup> Michel Laguerre,<sup>†</sup> Sabine Castano,<sup>†</sup> Bernard Desbat,<sup>†</sup> Dominique Cavagnat,<sup>‡</sup> Eric Ennifar,<sup>§</sup> Brice Kauffmann,<sup>||</sup> and Gilles Guichard<sup>\*,†</sup>

<sup>†</sup>Université de Bordeaux-CNRS UMR 5248, CBMN, Institut Européen de Chimie et Biologie, 2 rue Robert Escarpit, 33607 Pessac, France

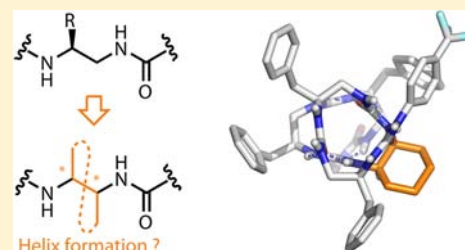
<sup>‡</sup>ISM, UMR CNRS 5255, Université de Bordeaux, 351 cours de la Libération, 33405 Talence, France

<sup>§</sup>Université de Strasbourg-CNRS UPR 9002, Architecture et Réactivité de l'ARN, IBMC, CNRS, 15 rue René Descartes, 67084 Strasbourg, France

<sup>||</sup>Université de Bordeaux-CNRS UMS 3033, INSERM US001, Institut Européen de Chimie et Biologie, 2 rue Robert Escarpit, 33607 Pessac, France

## Supporting Information

**ABSTRACT:** Aliphatic N,N'-linked oligoureas are peptidomimetic foldamers that adopt a well-defined helical secondary structure stabilized by a collection of remote three-center H-bonds closing 12- and 14-membered pseudoring. Delineating the rules that govern helix formation depending on the nature of constituent units is of practical utility if one aims to utilize this helical fold to place side chains in a given arrangement and elaborate functional helices. In this work, we tested whether the helix geometry is compatible with alternative substitution patterns. The central  $-\text{NH}-\text{CH}(\text{R})-\text{CH}_2-\text{NH}-\text{CO}-$  residue in a model oligourea pentamer sequence was replaced by guest units bearing various substitution patterns [e.g.,  $-\text{NH}-\text{CH}_2-\text{CH}_2-\text{NH}-\text{CO}-$ ,  $-\text{NH}-\text{CH}_2-\text{CH}(\text{R})-\text{NH}-\text{CO}-$ , and  $-\text{NH}-\text{CH}(\text{R}^1)-\text{CH}(\text{R}^2)-\text{NH}-\text{CO}-$ ], levels of preorganization (cyclic vs acyclic residues), and stereochemistries, and the helix formation was systematically assessed. The extent of helix perturbation or stabilization was primarily monitored in solution by Fourier transform IR, NMR, and electronic circular dichroism spectroscopies. Our results indicate that although three new substitution patterns were accommodated in the 2.5-helix, the helical urea backbone in short oligomers is particularly sensitive to variations in the residue substitution pattern (position and stereochemistry). For example, the *trans*-1,2-diaminocyclohexane unit was experimentally found to break the helix nucleation, but the corresponding *cis* unit did not. Theoretical calculations helped to rationalize these results. The conformational preferences in this series of oligoureas were also studied at high resolution by X-ray structure analyses of a representative set of modified oligomers.



## INTRODUCTION

The formation of stable and regular secondary structures maintained by remote intramolecular H-bonds (e.g., helices) requires preorganization of the main chain to position sequentially remote H-bond donors and acceptors in close spatial vicinity to enable optimal H-bonding to occur without significant conformational alteration. In natural  $\alpha$ -polypeptides, preferred backbone conformations derive in part from the minimization of eclipsing or Pitzer strain and pseudoallylic A(1,3) strain.<sup>1</sup> By analogy, restricted rotation about main-chain C–C bonds is a key feature that drives helical folding of higher  $\beta$ - and  $\gamma$ -peptide homologues.<sup>2–9</sup> For example, both canonical 14-helical structures of  $\beta^3$ - and  $\gamma^4$ -peptides are characterized by a (+)-synclinal arrangement (gauche conformation) around main-chain ethane bonds. Substantial stabilization of these helical folds has been achieved by increasing the level of preorganization of  $\beta$ - and  $\gamma$ -amino acid constituents toward the gauche conformation. In the  $\beta$ -peptide series, the *trans*-2-aminocyclohexyl carboxylic acid (*trans*-ACHC) unit<sup>10–12</sup> and

acyclic  $\beta^{2,3}$ -amino acids of like configuration<sup>13,14</sup> were found to be more effective than their  $\beta^3$  or  $\beta^2$  counterparts in promoting the requisite synclinal arrangement around  $\text{C}_\alpha-\text{C}_\beta$  bonds. Similarly, adding substituents at the 2-position (like configuration) or at both the 2- and 3-positions in  $\gamma^4$ -amino acid monomers was found to reduce significantly the number of conformations devoid of *syn*-pentane interactions and to reinforce optimal preorganization for 14-helix formation.<sup>15–17</sup> It is noteworthy that the exploration of substitution patterns can lead to the discovery of alternative folding patterns.  $\beta$ -Peptides consisting of the *trans*-2-aminocyclopentyl carboxylic acid (*trans*-ACPC)<sup>18,19</sup> and *trans*-2-aminocyclobutyl carboxylic acid (*trans*-ACBC)<sup>20</sup> adopt a stable 12-helix with a 1 $\leftarrow$ 4 H-bonding pattern that differs markedly from the 14-helix and associated 1 $\rightarrow$ 3 H-bonding scheme. In addition, a unique  $\beta$ -peptide 12,10-helical structure remote from the canonical 12-

Received: February 1, 2013

Published: February 27, 2013

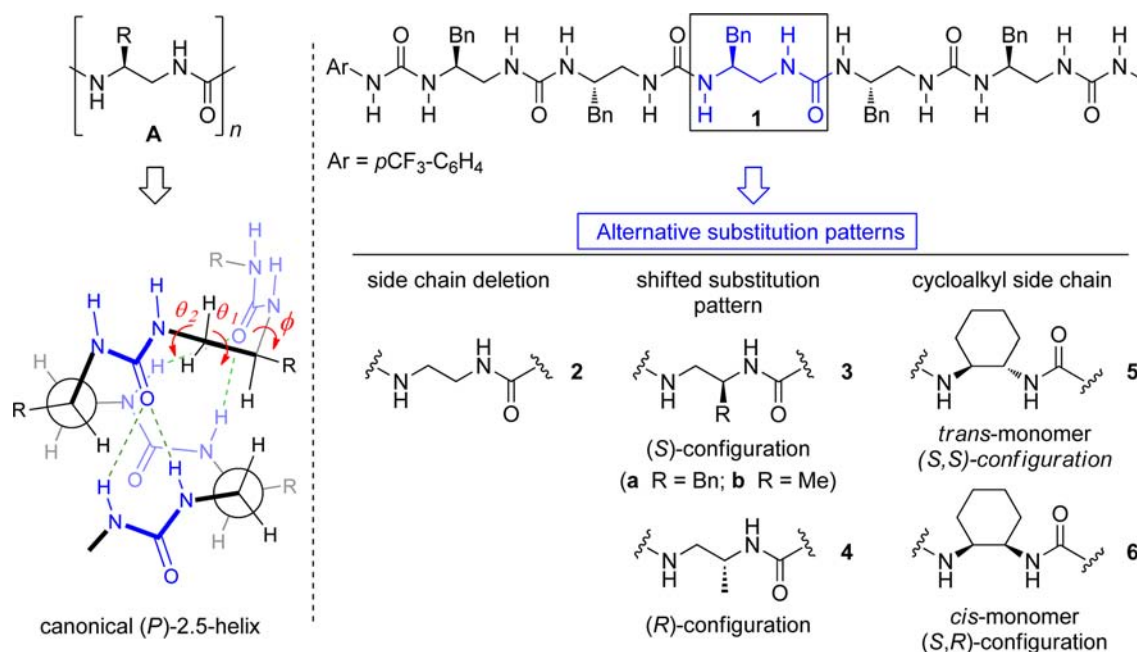


**Figure 1.** (left) Illustration of the canonical (*P*)-2.5-helical structure formed by *N,N'*-linked aliphatic oligoureas of type **A** together with the nomenclature used for the main-chain torsion angles:  $\text{OC-N-C}_\beta\text{-C}_\alpha$  is  $\phi$ ,  $\text{N-C}_\beta\text{-C}_\alpha\text{-N}$  is  $\theta_1$ , and  $\text{C}_\beta\text{-C}_\alpha\text{-N-CO}$  is  $\theta_2$ . (right) Sequences of model urea pentamer **1** (canonical units with the *S* configuration) and the alternative substitution patterns evaluated in this study.

and 14-helices has been reported for “mixed”  $\beta$ -peptides consisting of alternating  $\beta^3$ - and  $\beta^2$ -amino acids.<sup>14,21,22</sup>

Restriction of the conformational freedom of the C–C bonds toward the gauche conformer is also a prerequisite for helical folding in a family of aliphatic *N,N'*-linked oligoureas<sup>23</sup> having the general formula  $[-\text{NHCH}(\text{R})\text{CH}_2\text{NHCO}-]_n$ . Homochiral oligomers as short as four urea linkages have been shown to fold into a well-defined helical structure with 2.5 residues per helical turn and a pitch (rise per turn) of 5.1 Å (Figure 1 left).<sup>24–26</sup> X-ray diffraction (XRD) analyses of oligoureas **A** revealed a (+)-synclinal arrangement (*g+* conformation) around the ethane bond with an average backbone  $\text{N-C}_\beta\text{-C}_\alpha\text{-N}$  torsion angle ( $\theta_1$ ) of  $+57.8^\circ$ .<sup>27</sup> The helix is stabilized by a collection of three-center H-bonds closing 12- and 14-atom pseudorings. The chain-length dependence, the effect of capping, and the influence of the solvent on helical folding have been investigated in previous studies.<sup>28,29</sup> However, relatively little information is available about the folding propensity of units with alternative substitution patterns and their compatibility with the 2.5-helix geometry of oligoureas.<sup>30,31</sup> We recently reported a fragment condensation approach to long oligourea sequences and found that *N*-(pyrrolidine-2-ylmethyl)ureido units can be inserted at discrete positions without compromising 2.5-helical folding despite the loss of one H-bond donor site.<sup>30</sup> The conformational restriction around the  $\text{N-CH}(\text{R})$  bond imposed by the pyrrolidine ring fixes the  $\text{CO-N-C}_\beta\text{-C}_\alpha$  angle ( $\phi$ ) to a value of approximately  $-95.9^\circ$ , which matches the one found in the canonical structure of 2.5-helical oligoureas (i.e.,  $\phi \approx -101^\circ$ ). In the present work, we explored how the helix propensity is influenced by alternative ethylenediamine monomers with noncanonical substitution patterns and various conformational constraints (Figure 1 right). To assess the extent to which these monomers disrupt or stabilize the canonical 2.5-helical structure of oligoureas, we prepared singly substituted analogues of the model pentamer **1**. The folding behaviors of these short

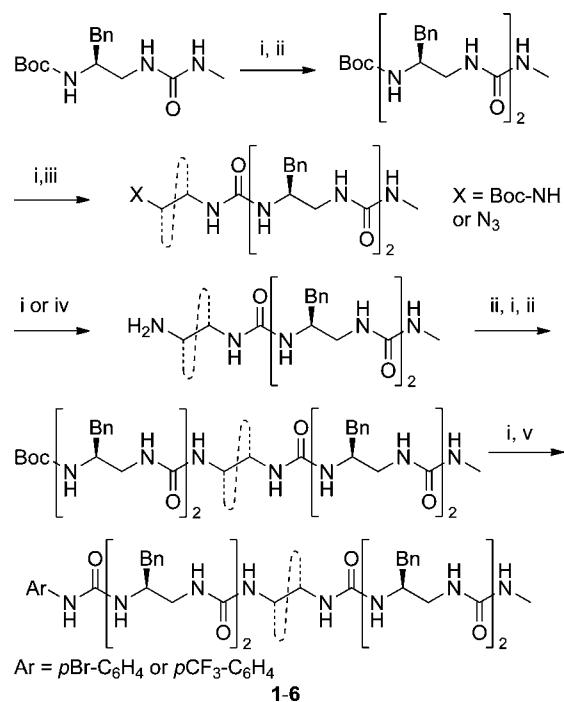
oligomers (**2–6**) were investigated using different experimental approaches, including Fourier transform IR (FTIR), electronic circular dichroism (ECD), and  $^1\text{H}$  NMR spectroscopies and X-ray crystallography, and finally compared with that of **1**.

## RESULTS AND DISCUSSION

**Design and Synthesis.** The singly substituted analogues of oligourea pentamer **1** considered in this work are shown in Figure 1. The central  $-\text{NH-CH}(\text{R})\text{-CH}_2\text{-NH-CO-}$  unit was replaced by residues with deleted side chains as in **2**, residues with shifted side chains ( $\text{C}_\beta \rightarrow \text{C}_\alpha$ ) as in **3** and **4**, or rotationally restricted *trans*- and *cis*-1,2-diaminocyclohexane units as in **5** and **6**. Examination of the high-resolution structures of the 2.5-helices of oligoureas<sup>27,30,32</sup> reveals a number of interesting features. The mean value of  $\sim 60^\circ$  for  $\theta_1$  in the helical backbone matches well the corresponding values in crystal structures of acylated 1,2-diaminocyclohexane derivatives (mainly *trans*) reported in the literature,<sup>33–38</sup> thus suggesting that such monomers could fit in the 2.5-helix (e.g., **5** and **6**). Whereas the side chains (*R*) of the canonical monomeric units in **A** adopt an equatorial (lateral) orientation with respect to the helix axis, the two hydrogens on the adjacent methylene group both point in a more axial direction (Figure 1 left). Therefore, it is more difficult to predict which substitution on this carbon would be tolerated (i.e., **3** vs **4**; **5** vs **6**). To get a first hint about the folding propensities of monosubstituted pentamers **2–6**, we performed a Monte Carlo (MC) conformational analysis with the GB/SA continuum solvation model (see the Supporting Information). The conformational search was optimized (force field and solvent) with pentaurea **1**, and main clusters of conformations were compared to the previously reported crystal structure of **1**.<sup>39</sup> The best results were obtained with AMBER\* as the force field and water as the solvent. The lowest-energy cluster was a helical conformation with a root-mean-square deviation (RMSD) of 0.6 Å relative to the crystal structure of **1**. The second- and

third-lowest-energy clusters contained partially helical structures. In such short-chain helical oligomers, the flexibility at both termini reduces the stability of the helical states, and the terminal segments tend to unravel. In the case of the monosubstituted analogues 4, 5, and 6, low-energy clusters were nevertheless populated by helical conformations akin to the canonical 2.5-helix. In contrast, helical conformations were hardly present in the clusters of conformations from simulations of 2 and 3. This conformational search thus suggests that in short-chain oligoureas, (i) the 2.5-helix geometry might accommodate both *cis*- and *trans*-1,2-diaminocyclohexane units, (ii) unsubstituted ethylenediamine units destabilize helix formation, and (iii) the introduction of a side chain on  $C_\alpha$  is tolerated when combined with inversion of configuration. To address these possibilities experimentally, oligoureas 1–6 were synthesized in solution according to Scheme 1 using (*S*)-succinimidyl- $\{2-[(tert\text{-butoxycarbonyl})-$

Scheme 1. Synthesis of Oligoureas 1–6<sup>a</sup>

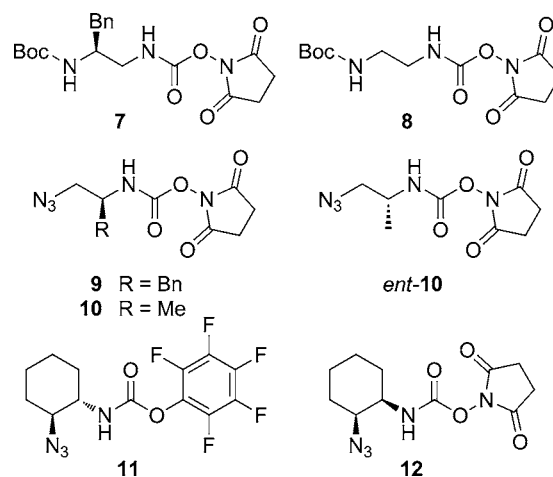


<sup>a</sup>Reagents and conditions: (i) TFA, 30 min; (ii) 7, DIPEA, MeCN, 2 h; (iii) 8–12, DIPEA, MeCN, 2 h; (iv) H<sub>2</sub>, Pd/C, 20% AcOH in MeOH, 2 h; (v) ArNCO, DIPEA, DMF or MeCN, 2 h. Abbreviations: DIPEA, diisopropylethylamine; TFA, trifluoroacetic acid; DMF, *N,N*-dimethylformamide.

amino]-3-phenylpropyl} carbamate (7) to introduce the canonical units. The overall yields of oligomers 2–6 ranged from 10 to 45% for the 10 steps (see the Supporting Information).

The specific building blocks 8–12 (whose preparation is described in the Supporting Information) were used to introduce residues with alternative substitution patterns (Chart 1). Briefly, activated carbamates 7–10 were prepared starting from *N*-Boc-protected amino acids using procedures previously described in the literature.<sup>40–42</sup> The *trans*- and *cis*-2-azidocyclohexyl carbamate monomers 11 and 12, respectively, were prepared from *trans*-2-aminocyclohexanol, which was obtained by catalytic asymmetric ring opening of cyclohexene oxide using the Jacobsen procedure.<sup>43</sup> The structure of 11 was

Chart 1. Activated Monomers 7–12 Used for the Synthesis of Oligoureas 1–6



unambiguously determined by XRD analysis (see the Supporting Information). After coupling of 11 and 12, reduction of the *cis*-2-azidocyclohexylurea intermediate to the corresponding amino derivative proved to be much more difficult than that of the corresponding *trans*-2-azidocyclohexylurea oligomer.

**FTIR Signatures of 1 and Analogues 2–6.** We first used FTIR spectroscopy as a rapid method to compare the different oligomers in both solution and the solid state. We previously showed that the FTIR spectra of helical oligoureas of type A are dominated by two strong bands centered near 1635 and 1570 cm<sup>-1</sup>. These two bands, which are essentially due to carbonyl stretching and coupled C–N stretching/N–H deformation are termed the “urea I” and “urea II” bands, respectively, by analogy to the amide I and amide II bands in peptides and proteins.<sup>44</sup>

In methanol solution (1–2 mg mL<sup>-1</sup>), the spectrum of model oligourea 1 (Figure 2a) displays the two intense urea I and urea II bands at 1633 cm<sup>-1</sup> (sharp) and 1583 cm<sup>-1</sup> (broader), respectively. As shown previously, the urea II region is more complex. It is split in two components, a strong one at 1583 cm<sup>-1</sup> and a shoulder at 1554 cm<sup>-1</sup>, corresponding to the coupled C–N stretching/N–H deformation with the two vibrational components in phase and out of phase, respectively. The additional band at 1602 cm<sup>-1</sup> is probably a contribution from the phenyl rings. The solution spectra of oligomer analogues 2, 4, and 6 (Figure 2c,d,f) display a common signature with an intense, sharp urea I band around 1630 cm<sup>-1</sup> that suggests folding. Very similar spectra were obtained in the solid state, suggesting that there is no major conformational change in going from solution to the solid state (see Table 1 and the spectra in the Supporting Information). Conversely, the solution spectra obtained for oligoureas 3b and 5 (Figure 2b,e) show extremely broad urea I and urea II bands with a shift of the urea I band toward higher wavenumber. The band broadening, which is even more pronounced in the solid state, does not support helical folding but rather reflects strong intermolecular interactions and aggregation behavior of these two oligomers. Overall, these FTIR results support the idea that the noncanonical units in 2, 4, and 6 but not those in 3 and 5 would be compatible with a 2.5-helix geometry.

**Folding Propensity in Solution As Determined by <sup>1</sup>H NMR Spectroscopy.** Additional information about the extent of helix perturbation or stabilization induced by the non-

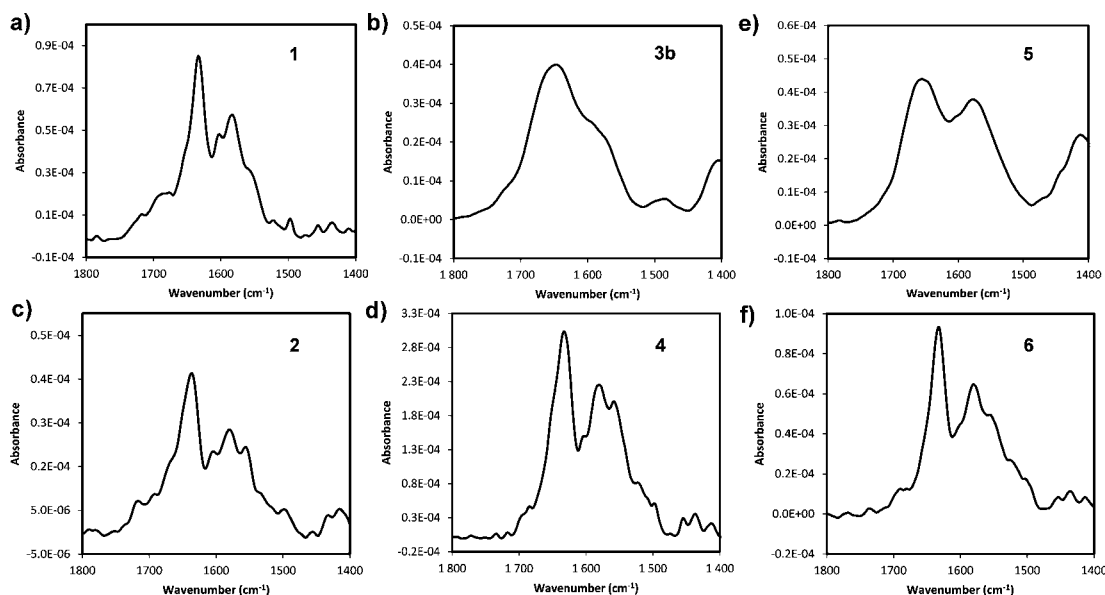


**Figure 2.** FTIR spectra (1400–1800  $\text{cm}^{-1}$ ) of oligoureas 1–6 recorded at room temperature in MeOH solution after subtraction of the spectrum of pure MeOH.

**Table 1.** C=O Stretching Frequencies for Oligomers 1–6 in Solution and the Solid State

compound	solution <sup>a</sup>		solid state	
	urea I	urea II	urea I	urea II
1	1633(s)	1583(m), 1554(sh)	1631(s)	1571(m), 1549(sh)
2	1638(m)	1580(m), 1555(m)	1635(s)	1578(s), 1556(sh)
3b	1647(m, br)	1591(sh)	1642(m, br)	1565(m, sh)
4	1633(s)	1578(s), 1558(s)	1634(s)	1576(m), 1555(sh)
5	1655(m, br)	1577(m, br)	1630(m)	1562(m, br)
6	1631(s)	1580(s), 1554(m, sh)	1630(s)	1572(m), 1555(m)

<sup>a</sup>Stretching frequencies in MeOH (1 or 2  $\text{mg mL}^{-1}$ ). Abbreviations: s, strong absorption; m, medium absorption; br, broad; sh, shoulder.

canonical units in oligomers 2–6 was gained by  $^1\text{H}$  NMR spectroscopy in  $\text{CD}_3\text{OH}$  at a concentration of 1 or 2 mM. We have shown that when placed in a helical environment, the main-chain methylene protons of canonical units exhibit a high degree of anisochronicity ( $\Delta\delta \geq 0.9$ –1 ppm for central residues). Thus, the  $\Delta\delta$  values can be used to sense the extent of helix perturbation. Herein, the  $\Delta\delta$  values for unmodified residues (i.e., residues 1, 2, 4 and 5) were extracted from  $^1\text{H}$  NMR spectra of oligomers 2–8 and compared to the corresponding values in 1 (Figure 3). The insertion of an achiral  $-\text{NH}-\text{CH}_2-\text{CH}_2-\text{NH}-\text{CO}-$  unit in 2 results in a lower degree of anisochronicity of the methylene protons (by  $\sim 0.2$  ppm relative to 1) in each of the four canonical units. The  $\Delta\delta$  value for the central unsubstituted residue is 0.45 ppm lower than that of the corresponding canonical chiral unit in 1. Overall, these lower  $\Delta\delta$  values may reflect either destabilization of the helical structure or some local adjustment of the helix geometry. Shifting the side chain on the adjacent backbone carbon atom without configurational reversal as in 3a (in which all of the residues have the *S* configuration) resulted in a completely different outcome. The  $^1\text{H}$  NMR spectra of 3a in  $\text{CD}_3\text{OH}$  were poorly resolved, and an unambiguous sequence assignment was precluded by significant overlap of the resonances in the NH region. Nevertheless, all of the spin systems could be resolved, and very limited diastereotopicity of main-chain methylene protons was found ( $\Delta\delta = 0.09$ –0.33 ppm). Substitution of a methyl group for the bulky benzyl side

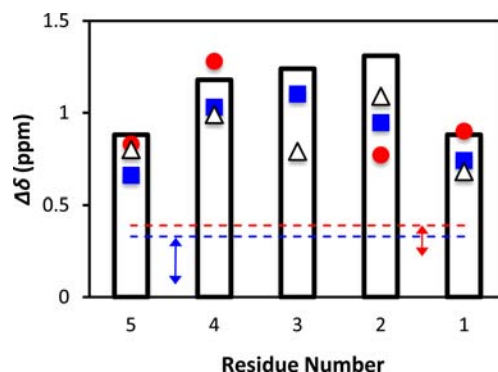


**Figure 3.** Anisochronicities ( $\Delta\delta$  in ppm) of the main-chain methylene protons of each residue in oligourea 1 (white bars) and the singly substituted analogues 2 (white  $\triangle$ ), 4 (blue  $\blacksquare$ ), and 6 (red  $\bullet$ ) measured in  $\text{CD}_3\text{OH}$  (1–2 mM; 400, 500, or 700 MHz; 298 K). Because the sequence assignment could not be inferred from the NMR spectra of compounds 3a and 5 (see the text), only the range of chemical shifts is indicated (blue arrow for 3a and red arrow for 5). The maximum  $\Delta\delta$  values measured for 3a and 5 are indicated by blue and red dashed lines, respectively.

chain in 3a did not yield any improvement, and 3b was not fully soluble in  $\text{CD}_3\text{OH}$  at 1 mM. In agreement with the MC simulations and FTIR data, coupling of a shift of the stereogenic center with inversion of configuration as in 4 (where the central unit has the *R* configuration) was found to

restore a high degree of anisochronicity in the flanking canonical units ( $\Delta\delta = 0.66$ – $1.10$  ppm), possibly suggesting 2.5-helical folding. The finding that the (*S,S*)-1,2-diaminocyclohexane unit is not accommodated in the 2.5-helix was not anticipated on the basis of the MC search but is consistent with the FTIR results. This substitution pattern in **5** led to major conformational changes, as shown by the significantly reduced anisochronicity along the backbone ( $\Delta\delta = 0.23$ – $0.39$  ppm). As in **3b**, the NH resonances in **5** were poorly dispersed, precluding identification of NH(*i*)/N'H(*i*+1) nuclear Overhauser effect (NOE) cross-peaks and subsequent sequence assignment. Interestingly, the (*S,R*)-1,2-diaminocyclohexane unit was able to maintain high  $\Delta\delta$  values in **6**, suggesting that the *cis*-1,2-diaminocyclohexane unit is compatible with the 2.5-helix geometry while the *trans* isomer is not.

The presence of nonsequential NOEs between backbone NH(*i*)/N'H(*i*) and C <sub>$\beta$</sub> H(*i*+2) (see the Supporting Information) provided further qualitative evidence that oligomers **2**, **4**, and **6**, like **1**, can adopt a helical conformation. However, the extraction of full NOE data sets for detailed NMR characterization and head-to-head comparisons of these short oligomers was hampered by the redundancy of benzyl side chains and numerous resonance overlaps in their NH/CH fingerprint regions. Measurement of amide proton exchange in proteins and  $\alpha$ -peptides is another established method to obtain useful structural information (stability, dynamics) at the residue level.<sup>45,46</sup> In the field of foldamers, this approach was recently used to compare the relative stabilities of short  $\alpha,\beta$ -peptide helices (nucleated or not) using the H-bond surrogate (HBS) technique.<sup>47</sup> By analogy to oligoamides, we investigated hydrogen/deuterium (H/D) exchange of backbone ureas in oligourea helices **2**, **4**, and **6** in comparison with **1** (Figure 4; also see the Supporting Information). Although a precise determination of the H/D exchange rates for all of the individual ureas was not possible because of overlaps in the 1D and 2D <sup>1</sup>H spectra, useful information was gained from the exchange data for few representative residues with NH protons putatively involved in intramolecular H-bonding. For example, the NH urea protons of residues 1 and 3 in **1** and **6** have exchange rates on the same order of magnitude ( $k_{\text{ex}} \leq 10 \times 10^{-3} \text{ min}^{-1}$ ). These protons exchange significantly more slowly than those in **2** and **4** ( $25 \times 10^{-3} \text{ min}^{-1} \leq k_{\text{ex}} \leq 44 \times 10^{-3} \text{ min}^{-1}$ ), thus suggesting a higher folding propensity for this region in **1** and **6** than in **2** and **4**.

**ECD Spectroscopy.** It has been shown that N,N'-linked oligoureas of type **A** display a characteristic ECD signature with an intense maximum at  $\sim 203$  nm upon (*P*)-2.5-helix formation.<sup>28</sup> Additional spectral characteristics of helix formation include a zero crossing at  $\sim 193$  nm and a minimum at 188 nm, which can be observed in trifluoroethanol (TFE) in the absence of aromatic side chains.<sup>30</sup> The ECD spectra of oligomers **1**–**6** ( $10^{-4}$  M in TFE) are shown in Figure 5. The poor ECD signal exhibited by oligoureas **3b** and **5** reflects the absence of a well-defined folded conformation, in line with the NMR and FTIR data. In contrast, oligomers **1**, **2**, **4**, and **6** all display an ECD signature with a maximum in the positive molar ellipticity at  $\sim 203$  nm, indicative of 2.5-helical folding. This is also consistent with the FTIR and NMR results. The negative band at 188 nm and the zero crossing at 193 nm are not visible in these spectra because they are masked by the positive contribution of the benzyl side chains.<sup>48</sup> Nevertheless, the intensities of the signals at 203 nm were tentatively used to compare the helix-folding propensities of the different

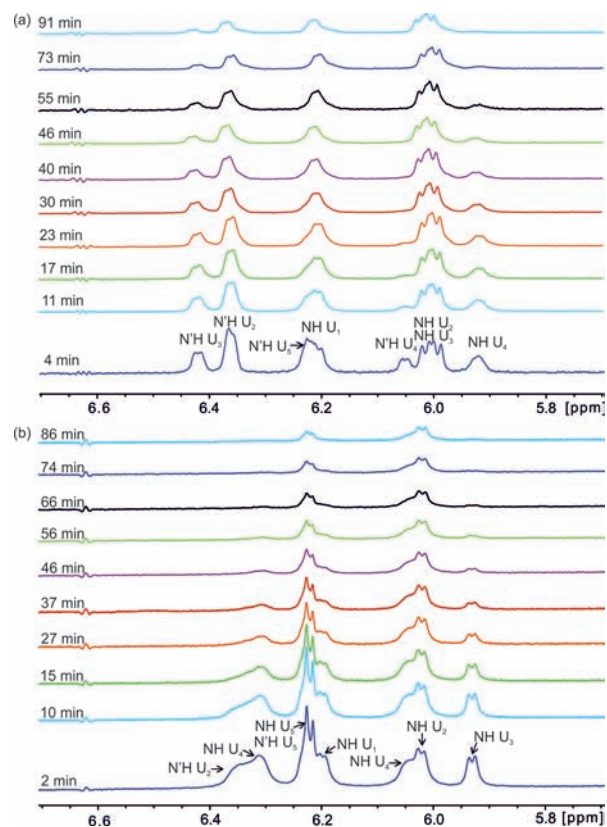


**Figure 4.** H/D exchange of backbone urea protons in (a) oligourea **1** and (b) oligourea **4**. The <sup>1</sup>H spectra (800 MHz) of the oligoureas (**1** mM in CD<sub>3</sub>OD) were recorded at 288 K.

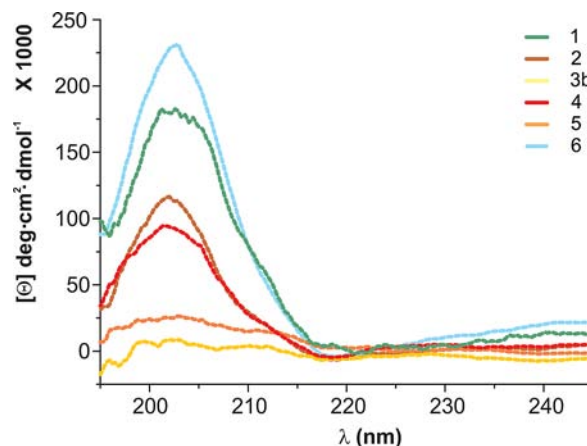


**Figure 5.** ECD spectra of oligoureas **1**–**6** ( $10^{-4}$  M in TFE) at 298 K.

oligomers qualitatively. The ECD signals exhibited by **2** and **4** are significantly weaker than that of **1**, indicating that the absence of a substituent or the shift of the side chain from C <sub>$\beta$</sub>  to C <sub>$\alpha$</sub>  in the central unit is destabilizing to some extent. In contrast, the intensity of the positive band at 203 nm for **6** is higher than that for **1**, suggesting that the insertion of a constrained *cis*-1,2-diaminocyclohexane unit is well-tolerated and stabilizes 2.5-helix formation to some extent in comparison with canonical acyclic units.

**X-ray Crystallographic Analysis.** To gain detailed structural insight into the consequences of incorporating noncanonical residues into oligoureas, we attempted to grow single crystals of oligomers **2**–**6** suitable for XRD analysis. We

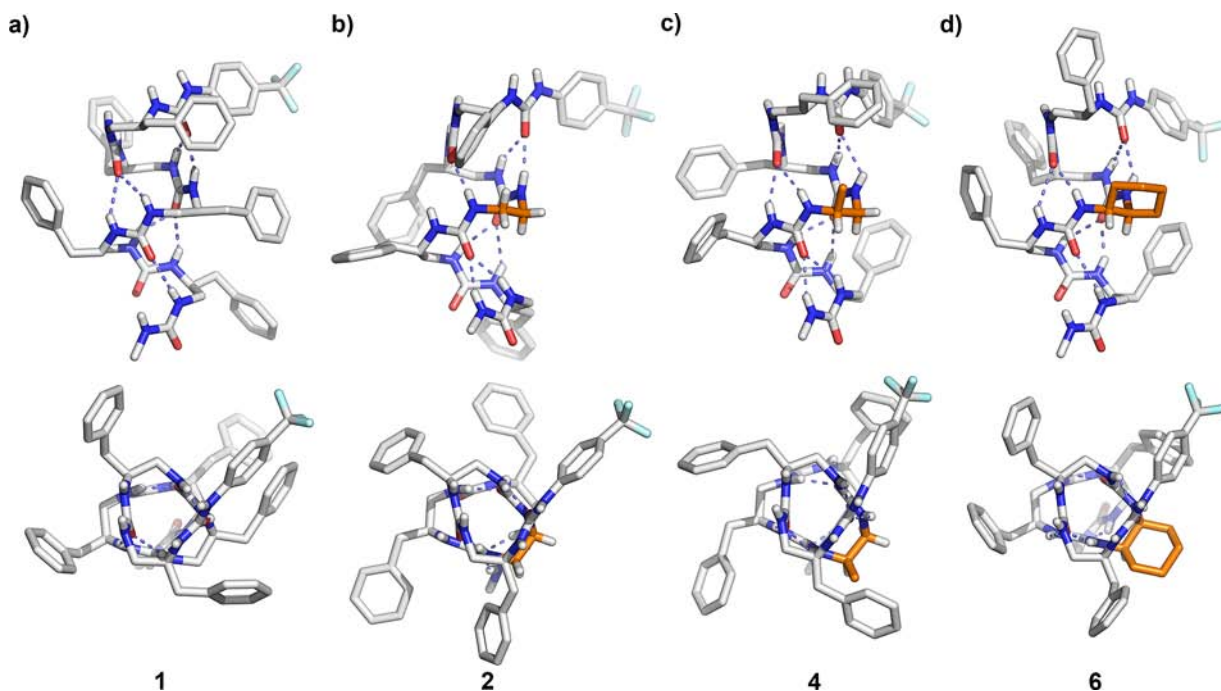


**Figure 6.** Comparison of the structures of oligoureas **1**, **2**, **4**, and **6** in the crystalline state: (top) side views; (bottom) top views. C atoms of the noncanonical units in **2**, **4**, and **6** are depicted in orange.

succeeded only in those cases where the new substitution pattern was shown by the FTIR, NMR, and ECD data to be compatible with 2.5-helical folding (i.e., for **2**, **4**, and **6**). Crystal structures of **2**, **4**, and **6** were solved in the  $P2_12_12_1$  (**2**) and  $P2_1$  (**4** and **6**) space groups (see the Supporting Information) and compared to the previously solved structure of **1**.<sup>39</sup> As shown in Figure 6, all three oligomers adopt a helical conformation akin to the canonical (*P*)-2.5-helical structure of **1**, thus confirming the results obtained in solution. Overlays of the structures of **2**, **4**, and **6** with that of **1** were performed by fitting the five pairs of  $\beta$ -carbons [CH(R) in the canonical units]. The low RMSDs of 0.342, 0.380, and 0.241 Å for **2**, **4**(I), and **6**(I), respectively, indicate a close match between the structures of the oligoureas with noncanonical residues and that of **1**. The intramolecular H-bond distances are also largely conserved among the four structures. As shown in Table 2, the modified residues accommodate the (*P*)-helix geometry with backbone torsion angles nearly identical to that of the central canonical unit in **1**.

**Table 2. Main Backbone Torsion Angles (deg) of the Central Canonical Unit in 1 and the Modified Units in Oligomers 2, 4, and 6 (from Crystal Structures)**

oligomer	$\phi$	$\theta_1$	$\theta_2$
<b>1</b>	-101.4	+54.4	+77.6
<b>2</b>	-90.0	+53.6	+79.2
<b>4</b> <sup>a</sup>	-98.6	+51.6	+83.7
<b>6</b> <sup>b</sup>	-95.3	+52.9	+82.9

<sup>a</sup>Means of the angles in the four independent molecules I–IV in the asymmetric unit (ASU). <sup>b</sup>Means of the angles in the two independent molecules I and II in the ASU.

An overlay of the *cis*-bis(ureido)cyclohexane unit at position 3 in **6** (C atoms in orange) with the corresponding canonical acyclic unit in **1** is shown in Figure 7. The backbone carbon

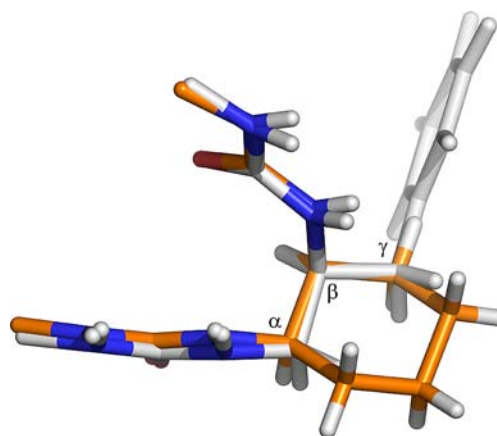


**Figure 7.** Overlay of the *cis*-bis(ureido)cyclohexane unit at position 3 in the crystal structure of **6** (C atoms in orange) with the corresponding canonical unit in the crystal structure of **1** (C atoms in light gray).

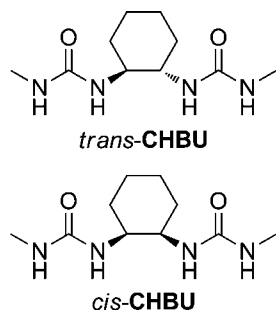
atoms and the first carbon of the side chain ( $C_\gamma$ ) show very little deviation between the two molecules, thus further highlighting the ability of a six-membered ring to match the helical backbone conformation of canonical acyclic units. It is also noteworthy that the introduction of discrete noncanonical units with substitution on  $C_\alpha$  leads to a different spacing and orientation of the side chains at the surface of the 2.5-helix. For example, the distances between the  $i$ ,  $i + 2$ , and  $i + 4$  side chains vary from 5.5 and 6.4 Å in **1** to 8.0 and 4.5 Å in **4** (see the Supporting Information).

**Substitution Pattern Requirements for 2.5-Helix Formation: Why *cis*- and Not *trans*-1,2-Diaminocyclo-**

**hexane Monomers?** The opposite nature of the *trans*- and *cis*-1,2-bis(ureido)cyclohexane units in **5** and **6**, respectively, as well as the central (*S*)- and (*R*)-1,2-bis(ureido)propane units in **3** and **4**, respectively, is not easily inferred from examination of the model shown in Figure 1 but can eventually be rationalized by considering the torsion angle preferences in these units. Examination of the torsion angles of (*S*)-2-substituted-1,2-diaminoethane units in the crystal structures of model mono- and diureas [e.g., (*S*)-Bn-NHCONH-CH(Bn)-CH<sub>2</sub>-NHCONH-Me]<sup>49</sup> and helical oligoureas<sup>27,30</sup> revealed that, as in L-peptides, the OC-N-C<sub>β</sub>-C<sub>α</sub> angle  $\phi$  adopts negative values. This preference for negative  $\phi$  values in canonical units having the *S* configuration may thus suggest that shifting the substitution position to the second carbon while keeping the configuration constant, as in **3**, may locally impose negative values of the C<sub>β</sub>-C<sub>α</sub>-N-CO angle  $\theta_2$  and thus an antiparallel orientation of the ureas, precluding *P*-helical folding despite the presence of flanking canonical units. Combining a shift of the substitution position with inversion of configuration, as in **4**, would then restore helical folding by allowing the central unit to adopt a positive  $\theta_2$  value. This may also hold true for the (*S,S*)-*trans*- and (*S,R*)-*cis*-1,2-diaminocyclohexane units in **5** and **6**, respectively.

To test this hypothesis and gain additional information about conformational preferences of (1*S*,2*S*)-*trans*- and (1*S*,2*R*)-*cis*-1,2-bis(ureido)cyclohexane units, we performed theoretical calculations on the model compounds *trans*- and *cis*-1,1'-(cyclohexane-1,2-diyl)bis(3-methylurea) (CHBU) (Chart 2).

**Chart 2. Model *trans*- and *cis*-1,2-Bis(ureido)cyclohexane Derivatives Used in the Calculations**



The entire conformational energy surface of the two molecules was first sampled by carrying out semiempirical calculations using the RM1 method<sup>50</sup> with the simulated annealing technique implemented in Ampac 9.<sup>51</sup> The search for the various local minima on this surface was performed in two stages: (i) a nonlocal search focused on 18 dihedral angles corresponding to the torsions defining the different conformers and (ii) a local energetic relaxation of all of the degrees of freedom for each of the minima collected at each stage. In this way, 30–50 conformers with energies within 8–10 kcal/mol of the lowest-energy conformer were determined (see the Supporting Information). The *trans* diastereomer (−116.7 kcal mol<sup>−1</sup>) was calculated to be more stable than the *cis* one (−114.1 kcal mol<sup>−1</sup>). For *trans*-CBHU, the anti conformation (i.e., negative values of  $\phi$  and  $\theta_2$ ; ureas pointing in opposite directions) was found to be more stable than the *syn* conformation (i.e., negative  $\phi$  and positive  $\theta_2$  values) by 5.8 kcal/mol. A *syn* conformation was found to be more stable for *cis*-CBHU (−113.8 kcal mol<sup>−1</sup>), but the difference in the

energies of the two conformers was smaller ( $\Delta H_{\text{syn-anti}} = -1.2$  kcal mol<sup>−1</sup>).

Geometry optimizations were performed using density functional theory with the wB97XD functional<sup>52</sup> and the 6-31G\*\* basis set starting from the low-energy *syn* and *anti* conformers identified in the semiempirical calculations. The results (Figure 8) are consistent with those of semiempirical

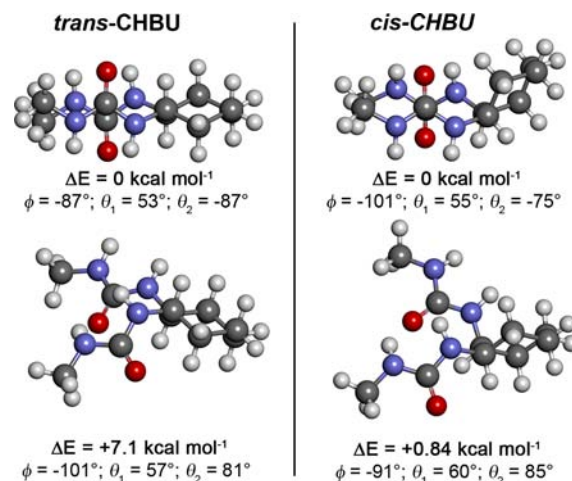


**Figure 8.** Optimized geometries of (top) the anti conformers (negative values of  $\phi$  and  $\theta_2$ ) and (bottom) the *syn* conformers (negative  $\phi$  and positive  $\theta_2$  values) of (left) *trans*- and (right) *cis*-CHBU.

annealing. For both *trans*- and *cis*-CHBU, the anti conformation is the more energetically stable. However, the energy difference between the anti and *syn* conformers is significantly smaller for *cis*-CHBU (0.8 kcal mol<sup>−1</sup>) than for *trans*-CHBU (6.8 kcal mol<sup>−1</sup>). Altogether, these calculations suggest that a *syn* conformation is accessible at a lower energetic cost for the *cis*-1,2-diaminocyclohexane derivatives. Furthermore, the values of the backbone torsion angles in the optimized *syn* conformation of *cis*-CHBU ( $\phi = -91^\circ$ ;  $\theta_1 = 60^\circ$ ;  $\theta_2 = 85^\circ$ ) match well the backbone torsion angles of the 2.5-helix geometry.

Finally, we screened the  $\phi$  versus  $\theta_2$  energy surfaces of *trans*- and *cis*-CHBU by scanning  $\phi$  and  $\theta_2$  in steps of 18°. The  $\phi$  versus  $\theta_2$  energy contours (Ramachandran-type plots) calculated at the wB97XD/6-31G\*\* level are provided in the Supporting Information. We observed that (i) both *cis*- and *trans*-CHBU have several minima in the region corresponding to negative values of  $\phi$  and  $\theta_2$  [e.g., ( $\phi, \theta_2$ ) = (−100°, −80°), (−150°, −80°), and (−90°, −160°)] and (ii) only *cis*-CHBU exhibits minima with positive values of  $\theta_2$  [e.g., (−90°, 80°)].<sup>53</sup> Overall, these results are in good agreement with the finding that *cis*- but not *trans*-1,2-diaminocyclohexane-type units are accommodated in the short 2.5-helices reported here.

## CONCLUSION

We have investigated the extent to which the helical conformation of short aliphatic peptidomimetic oligoureas is affected by the substitution pattern and the relative configuration of ethylenediamine units. Similar to  $\beta$ -amino acids, the chiral ethylenediamine constituents of oligoureas are chemically and structurally diverse building blocks with six substitution positions (vs three for  $\alpha$ -amino acids) and eight possible configurational isomers (vs two for  $\alpha$ -amino acids).

The possibility of employing monomeric units with different substitution patterns and various degrees of preorganization may be useful for fine-tuning the arrangement of functional groups at the helix surface, modulating the helix stability, and ultimately enabling the design of more effective peptide mimics and/or sophisticated folded architectures (e.g., helical bundles<sup>54,55</sup>).

Our solution and solid-state data demonstrate that the constrained *cis*-1,2-diaminocyclohexane-type unit is readily accommodated in the 2.5-helix environment. The backbone torsion angles  $\phi$ ,  $\theta_1$ , and  $\theta_2$  of the cycloalkyl unit in **6** closely match those of the acyclic residues in the canonical 2.5-helix formed by homo-oligomers (e.g., **1**). The enhancement of helical folding by cyclic residues is well-documented among  $\beta$ -peptide foldamers (e.g., stabilization of the 14-helix by *trans*-AACH residues).<sup>56–58</sup> Our spectroscopic measurements indicate that oligomers **1** and **6** both adopt a stable helical structure, with the ECD spectra providing some support for an increase in helical content upon insertion of a central *cis*-1,2-diaminocyclohexane residue. However, the presence of benzyl side chains and their contribution to the far-UV ECD spectra of oligomers **1–6** may render a quantitative comparison of the ECD spectra more difficult. Interestingly, while this article was in preparation, short homo-oligomers made of even more constrained bicyclic units [i.e., (*S*)-bicyclo[2.2.2]octane-1,2-diamine] were reported.<sup>31</sup> The finding that these oligomers adopt a 2.5-helical conformation (though partially distorted in the crystal state of a tetramer) along with the results described here suggest that homo-oligomers composed (*S,R*)-*cis*-1,2-diaminocyclohexane units may also adopt a helical structure akin to that of **1** and **6**.

Calculations and experimental data also reveal that backbone torsion angle preferences in *trans*-1,2-diaminocyclohexane units favor an anti conformation (negative values of  $\phi$  and  $\theta_2$ ) with flanking ureas pointing in opposite directions, which is not compatible with the 2.5-helix geometry (at least in short-chain oligomers). One can speculate that repeats of this motif would rather generate extended conformations prone to the formation of  $\beta$ -sheet-type arrangements, akin to that of  $\beta$ -peptides of *cis*-aminocycloalkyl carboxylic acids, which adopt extended conformations.<sup>59</sup> In this work, we did not investigate cyclic units with smaller ring sizes such as 1,2-diaminocyclopentane and 1,2-diaminocyclobutane derivatives. It not clear whether the constraints imposed by smaller rings would support torsion angles associated with 2.5-helical folding. The anticipated preference for larger  $\theta_1$  values in four- and five-membered rings may instead promote alternative folding patterns in the corresponding homo-oligomers similar to what is observed for  $\beta$ -peptides. *trans*-ACPC and *trans*-ACBC residues in the  $\beta$ -peptide 12-helix environment are characterized by average N–C $_{\beta}$ –C $_{\alpha}$ –CO angles of 94 and 96°, respectively.<sup>20,60</sup>

Previous work on modified oligourea sequences incorporating noncanonical *N*-pyrrolidine units (proline-like residues)<sup>30</sup> or isosteric amide and carbamate units<sup>39</sup> has revealed the capacity of a few canonical urea monomers to impose their conformational preference on units with otherwise limited folding character. Our data indicate that units having no substituent (glycine-like) or combining a shift of the substitution position (C $_{\beta}$   $\rightarrow$  C $_{\alpha}$ ) with inversion of configuration (*S*  $\rightarrow$  *R*) can be substituted for the canonical units at discrete positions in the sequence, albeit with some destabilization of the 2.5-helical fold in such short oligomers. Nevertheless, the finding that the helix formed by units having the *S*

configuration tolerates the introduction in the reverse direction of units having the opposite configuration [i.e., intrinsically programmed to nucleate an (*M*)-2.5 helix] is intriguing and may be used to modulate the distribution of side chains at the surface of this helical fold. However, the maximum number of *R* units that can be inserted without causing global unfolding of the (*P*)-helix as well as authorized combinations (e.g., 1:1 pattern) still need to be determined precisely. It is worth mentioning that hybrid  $\beta$ -peptides composed of  $\beta^2/\beta^3$  dipeptide repeats (C $_{\beta}$   $\rightarrow$  C $_{\alpha}$  shift)<sup>14,21</sup> or heterochiral sequences [e.g., alternating (*S*)- $\beta^3$  and (*R*)- $\beta^3$  amino acid residues]<sup>61,62</sup> form mixed-helical structures (i.e., with alternating orientation of the backbone amides) that differ from the canonical  $\beta$ -peptide 14-helix. It remains to be seen whether oligoureas composed of heterochiral sequences would show a similar propensity to adopt noncanonical secondary structures.

## ■ ASSOCIATED CONTENT

### 📄 Supporting Information

Experimental methods, spectroscopic data, crystallographic information files (CIF), and  $\phi$  vs  $\theta_2$  energy contour plots. This material is available free of charge via the Internet at <http://pubs.acs.org>.

## ■ AUTHOR INFORMATION

### Corresponding Author

[g.guichard@iecb.u-bordeaux.fr](mailto:g.guichard@iecb.u-bordeaux.fr)

### Present Address

<sup>†</sup>N.P.: Departments of Chemistry and Biochemistry, University of Washington, Seattle, WA 98195, United States.

### Notes

The authors declare no competing financial interest.

## ■ ACKNOWLEDGMENTS

This work was supported by the Centre National de la Recherche Scientifique (CNRS), the Université de Bordeaux, and the Conseil Régional d'Aquitaine and by a grant from the Agence Nationale de la Recherche (ANR-07-PCVI-0018). A fellowship from the Université de Strasbourg (N.P.) is gratefully acknowledged. We also thank Immupharma France and ANRT for a CIFRE predoctoral fellowship to P.C. The authors also acknowledge computational facilities provided by the Pôle Modélisation of the Institut des Sciences Moléculaires. The crystallographic data were collected at the IECB X-ray facility (UMS 3033, CNRS and Université de Bordeaux, US 001 INSERM), the ESRF (Grenoble, France), and the Swiss Light Source (SLS) (Villigen, Switzerland). Beamline scientists from ESRF ID29 and SLS X06SA are warmly acknowledged for beamtime and help during data collection. We thank Vincent Olieric for his support at the SLS synchrotron and Axelle Grélard for her assistance with NMR measurements.

## ■ REFERENCES

- (1) Quinkert, G.; Egert, E.; Griesinger, C. *Aspects of Organic Chemistry: Structure*; Verlag Helvetica Chimica Acta: Basel, Switzerland, 1996.
- (2) Seebach, D.; Matthews, J. L. *Chem. Commun.* **1997**, 2015–2022.
- (3) Banerjee, A.; Balaran, P. *Curr. Sci.* **1997**, 73, 1067–1077.
- (4) Gellman, S. H. *Acc. Chem. Res.* **1998**, 31, 173–180.
- (5) Cheng, R. P.; Gellman, S. H.; DeGrado, W. F. *Chem. Rev.* **2001**, 101, 3219–3232.
- (6) Seebach, D.; Beck, A. K.; Bierbaum, D. J. *Chem. Biodiversity* **2004**, 1, 1111–1239.



- (7) Le Grel, P.; Guichard, G. In *Foldamers: Structure, Properties, and Applications*; Hecht, S., Huc, L., Eds.; Wiley-VCH: Weinheim, Germany, 2007; pp 35–74.
- (8) Martinek, T. A.; Fülöp, F. *Chem. Soc. Rev.* **2012**, *41*, 687–702.
- (9) Bouillère, F.; Thétiot-Laurent, S.; Kouklovsky, C.; Alezra, V. *Amino Acids* **2011**, *41*, 687–707.
- (10) Appella, D. H.; Christianson, L. A.; Karle, I. L.; Powell, D. R.; Gellman, S. H. *J. Am. Chem. Soc.* **1996**, *118*, 13071–13072.
- (11) Appella, D. H.; Christianson, L. A.; Karle, I. L.; Powell, D. R.; Gellman, S. H. *J. Am. Chem. Soc.* **1999**, *121*, 6206–6212.
- (12) Barchi, J. J.; Huang, X.; Appella, D. H.; Christianson, L. A.; Durell, S. R.; Gellman, S. H. *J. Am. Chem. Soc.* **2000**, *122*, 2711–2718.
- (13) Seebach, D.; Ciceri, P. E.; Overhand, M.; Jaun, B.; Rigo, D. *Helv. Chim. Acta* **1996**, *79*, 2043–2066.
- (14) Seebach, D.; Abele, S.; Gademann, K.; Guichard, G.; Hintermann, T.; Jaun, B.; Matthews, J. L.; Schreiber, J. V.; Oberer, L.; Hommel, U.; Widmer, H. *Helv. Chim. Acta* **1998**, *81*, 932–982.
- (15) Hanessian, S.; Luo, X.; Schaum, R.; Michnick, S. *J. Am. Chem. Soc.* **1998**, *120*, 8569–8570.
- (16) Seebach, D.; Brenner, M.; Rueping, M.; Schweizer, B.; Jaun, B. *Chem. Commun.* **2001**, 207–208.
- (17) Seebach, D.; Brenner, M.; Rueping, M.; Jaun, B. *Chem.—Eur. J.* **2002**, *8*, 573–584.
- (18) Appella, D. H.; Christianson, L. A.; Klein, D. A.; Powell, D. R.; Huang, X.; Barchi, J. J.; Gellman, S. H. *Nature* **1997**, *387*, 381–384.
- (19) Appella, D. H.; Christianson, L. A.; Klein, D. A.; Richards, M. R.; Powell, D. R.; Gellman, S. H. *J. Am. Chem. Soc.* **1999**, *121*, 7574–7581.
- (20) Fernandes, C.; Faure, S.; Pereira, E.; Théry, V.; Declerck, V.; Guillot, R.; Aitken, D. J. *Org. Lett.* **2010**, *12*, 3606–3609.
- (21) Seebach, D.; Gademann, K.; Schreiber, J. V.; Matthews, J. L.; Hintermann, T.; Jaun, B.; Oberer, L.; Hommel, U.; Widmer, H. *Helv. Chim. Acta* **1997**, *80*, 2033–2038.
- (22) Rueping, M.; Schreiber, J. V.; Lelais, G.; Jaun, B.; Seebach, D. *Helv. Chim. Acta* **2002**, *85*, 2577–2593.
- (23) Burgess, K.; Shin, H.; Linthicum, D. S. *Angew. Chem., Int. Ed. Engl.* **1995**, *34*, 907–909.
- (24) Fischer, L.; Guichard, G. *Org. Biomol. Chem.* **2010**, *8*, 3101–3117.
- (25) Semetey, V.; Rognan, D.; Hemmerlin, C.; Graff, R.; Briand, J.-P.; Marraud, M.; Guichard, G. *Angew. Chem., Int. Ed.* **2002**, *41*, 1893–1895.
- (26) Hemmerlin, C.; Marraud, M.; Rognan, D.; Graff, R.; Semetey, V.; Briand, J.-P.; Guichard, G. *Helv. Chim. Acta* **2002**, *85*, 3692–3711.
- (27) Fischer, L.; Claudon, P.; Pendem, N.; Miclet, E.; Didierjean, C.; Ennifar, E.; Guichard, G. *Angew. Chem., Int. Ed.* **2010**, *49*, 1067–1070.
- (28) Violette, A.; Averlant-Petit, M. C.; Semetey, V.; Hemmerlin, C.; Casimir, R.; Graff, R.; Marraud, M.; Briand, J.-P.; Rognan, D.; Guichard, G. *J. Am. Chem. Soc.* **2005**, *127*, 2156–2164.
- (29) Violette, A.; Lancelot, N.; Poschalko, A.; Piotta, M.; Briand, J. P.; Raya, J.; Elbayed, K.; Bianco, A.; Guichard, G. *Chem.—Eur. J.* **2008**, *14*, 3874–3882.
- (30) Fremaux, J.; Fischer, L.; Arbogast, T.; Kauffmann, B.; Guichard, G. *Angew. Chem., Int. Ed.* **2011**, *50*, 11382–11385.
- (31) Legrand, B.; André, C.; Wenger, E.; Didierjean, C.; Averlant-Petit, M. C.; Martinez, J.; Calmes, M.; Amblard, M. *Angew. Chem., Int. Ed.* **2012**, *51*, 11267–11270.
- (32) Guichard, G.; Violette, A.; Chassaing, G.; Miclet, E. *Magn. Reson. Chem.* **2008**, *46*, 918–924.
- (33) Andre, C.; Luger, P.; Nehmzow, D.; Fuhrhop, J. H. *Carbohydr. Res.* **1994**, *261*, 1–11.
- (34) Anthony, S. P.; Basavaiah, K.; Radhakrishnan, T. P. *Cryst. Growth Des.* **2005**, *5*, 1663–1666.
- (35) Qiao, J. X.; Chang, C.-H.; Cheney, D. L.; Morin, P. E.; Wang, G. Z.; King, S. R.; Wang, T. C.; Rendina, A. R.; Luettgen, J. M.; Knabb, R. M.; Wexler, R. R.; Lam, P. Y. S. *Bioorg. Med. Chem. Lett.* **2007**, *17*, 4419–4427.
- (36) Alfonso, I.; Bolte, M.; Bru, M.; Burguete, M. I.; Luis, S. V. *Chem.—Eur. J.* **2008**, *14*, 8879–8891.
- (37) Hanessian, S.; Vinci, V.; Fettes, K.; Maris, T.; Viet, M. T. P. *J. Org. Chem.* **2007**, *73*, 1181–1191.
- (38) Amendola, V.; Boiocchi, M.; Esteban-Gomez, D.; Fabbri, L.; Monzani, E. *Org. Biomol. Chem.* **2005**, *3*, 2632–2639.
- (39) Pendem, N.; Nelli, Y. R.; Douat, C.; Fischer, L.; Laguerre, M.; Ennifar, E.; Kauffmann, B.; Guichard, G. *Angew. Chem., Int. Ed.* **2013**, DOI: 10.1002/anie.201209838.
- (40) Kim, J.-M.; Bi, Y.; Paikoff, S. J.; Schultz, P. G. *Tetrahedron Lett.* **1996**, *37*, 5305–5308.
- (41) Guichard, G.; Semetey, V.; Didierjean, C.; Aubry, A.; Briand, J.-P.; Rodriguez, M. *J. Org. Chem.* **1999**, *64*, 8702–8705.
- (42) Aisenbrey, C.; Nagendar, P.; Guichard, G.; Bechinger, B. *Org. Biomol. Chem.* **2012**, *10*, 1440–1447.
- (43) Schaus, S. E.; Larrow, J. F.; Jacobsen, E. N. *J. Org. Chem.* **1997**, *62*, 4197–4199.
- (44) Cavagnat, D.; Claudon, P.; Fischer, L.; Guichard, G.; Desbat, B. *J. Phys. Chem. B* **2011**, *115*, 4446–4452.
- (45) Englander, S. W.; Mayne, L. *Annu. Rev. Biophys. Biomol. Struct.* **1992**, *21*, 243–265.
- (46) Goodman, E. M.; Kim, P. S. *Biochemistry* **1991**, *30*, 11615–11620.
- (47) Patgiri, A.; Joy, S. T.; Arora, P. S. *J. Am. Chem. Soc.* **2012**, *134*, 11495–11502.
- (48) Sreerama, N.; Manning, M. C.; Powers, M. E.; Zhang, J.-X.; Goldenberg, D. P.; Woody, R. W. *Biochemistry* **1999**, *38*, 10814–10822.
- (49) Fischer, L.; Didierjean, C.; Jolibois, F.; Semetey, V.; Lozano, J. M.; Briand, J. P.; Marraud, M.; Poteau, R.; Guichard, G. *Org. Biomol. Chem.* **2008**, *6*, 2596–2610.
- (50) Stewart, J. J. *Mol. Model.* **2007**, *13*, 1173–1213.
- (51) AMPAC 9; Semichem, Inc.: Shawnee, KS, 2008.
- (52) Chai, J.-D.; Head-Gordon, M. *Phys. Chem. Chem. Phys.* **2008**, *10*, 6615–6620.
- (53) The *D-pro-(S,R)-cis-1,2-diaminocyclohexane* unit has been used previously as a reverse-turn scaffold to connect short urea segments. In this case, the backbone torsion angles for the *cis-1,2-diaminocyclohexane* unit are  $\phi = -105^\circ$ ,  $\theta_1 = 56^\circ$ , and  $\theta_2 = 162^\circ$ . See: Medda, A. K.; Park, C. M.; Jeon, A.; Kim, H.; Sohn, J.-H.; Lee, H.-S. *Org. Lett.* **2011**, *13*, 3486–3489.
- (54) Daniels, D. S.; Petersson, E. J.; Qiu, J. X.; Schepartz, A. *J. Am. Chem. Soc.* **2007**, *129*, 1532–1533.
- (55) Giuliano, M. W.; Horne, W. S.; Gellman, S. H. *J. Am. Chem. Soc.* **2009**, *131*, 9860–9861.
- (56) Raguse, T. L.; Porter, E. A.; Weisblum, B.; Gellman, S. H. *J. Am. Chem. Soc.* **2002**, *124*, 12774–12785.
- (57) Raguse, T. L.; Lai, J. R.; Gellman, S. H. *J. Am. Chem. Soc.* **2003**, *125*, 5592–5593.
- (58) Seebach, D.; Jacobi, A.; Rueping, M.; Gademann, K.; Ernst, M.; Jaun, B. *Helv. Chim. Acta* **2000**, *83*, 2115–2140.
- (59) Martinek, T. A.; Tóth, G. K.; Vass, E.; Hollósi, M.; Fülöp, F. *Angew. Chem., Int. Ed.* **2002**, *41*, 1718–1721.
- (60) Choi, S. H.; Guzei, I. A.; Spencer, L. C.; Gellman, S. H. *J. Am. Chem. Soc.* **2010**, *132*, 13879–13885.
- (61) Sharma, G. V.; Reddy, K. R.; Krishna, P. R.; Sankar, A. R.; Narsimulu, K.; Kumar, S. K.; Jayaprakash, P.; Jagannadh, B.; Kunwar, A. C. *J. Am. Chem. Soc.* **2003**, *125*, 13670–13671.
- (62) Mándity, I. M.; Wéber, E.; Martinek, T. A.; Olajos, G.; Tóth, G. K.; Vass, E.; Fülöp, F. *Angew. Chem., Int. Ed. Engl.* **2009**, *48*, 2171–2175.